

Detection of pulsar beams deflected by the black hole in Sgr A*: effects of black hole spin

Sourabh Nampalliwar

Department of Physics & Astronomy and Center for Gravitational Wave Astronomy, University of Texas at Brownsville, Brownsville, Texas 78520

Richard H. Price, Teviet Creighton and Fredrick A. Jenet

Department of Physics & Astronomy, Center for Gravitational Wave Astronomy and Center for Advanced Radio Astronomy, University of Texas at Brownsville, Brownsville, Texas 78520

1. Introduction

It is believed that the center of essentially every large galaxy, including our own, contains a supermassive black hole (SMBH). Sagittarius A*, first discovered as a bright radio source, is expected to host the SMBH at the center of the Milky Way. Observations of the region in the infrared (Genzel et al. 2003; Gillessen et al. 2009), radio (Doeleman et al. 2008; Broderick et al. 2009), x-ray (Baganoff et al. 2003; Porquet et al. 2003) and optical (Ghez et al. 2008), have revealed properties of the central object such as mass and accretion flow. Alternates to an SMBH, such as a dense cluster of dark stellar objects or a ball of massive, degenerate fermions (Schödel et al. 2002) have largely been ruled out. These observations also indicate an initial mass function (IMF) near the SMBH strongly tilted towards massive stars (Nayakshin & Sunyaev 2005; Maness et al. 2007; Levin 2006). This top-heavy IMF suggests a large population of neutron stars orbiting the SMBH with estimates placing ~ 10000 of them within 1 pc of Sgr A* (Muno et al. 2005) and 1000 within 0.01 pc (Pfahl & Loeb 2004). Beams from these pulsars could traverse the strong field region of the SMBH, be deflected and reach the Earth. Using the precision of pulsar timing, we might be able to detect these deflected beams and from them infer properties of the strong field region through which the beams have passed.

Previous work in this direction with the assumption of a nonspinning SMBH has been reported in Wang et al. (Wang et al. 2009b,a) and Stovall et al. (Stovall et al. 2012) (hereafter Paper I, II and III respectively). In Paper I, strong field effects on the intensity and time of arrivals (TOA) of pulsar beams were analyzed in the case that the pulsar beam is confined to the plane of the pulsar orbit. Paper II extended the formalism to general orientations. In Paper III, an estimate was given of the probability of observing these deflected pulsar beams. For the pulsar luminosity distribution calculated in the ATNF Pulsar Catalog¹, it was found that there is a marginal probability of detection with current instruments, like the Parkes and Green Bank Telescope, and

¹<http://www.atnf.csiro.au/research/pulsar/psrcat/>

future instruments, in particular FAST and SKA, provide a reasonable chance of detection. For a more conservative distribution (Faucher-Giguère & Kaspi 2006), chances of detection with existing telescopes are weak, and we must await more sensitive instruments like SKA.

Paper III was based on the the model of Paper II, and hence embodied the assumption of a nonspinning SMBH. The Sgr A* SMBH is certainly expected to be rotating, though the rate of rotation is indeterminate, with predictions for the spin rate ranging from very slow (Liu & Melia 2002) to moderate (Genzel et al. 2003). In principle, spin effects could have a dramatic effect on beam bending and hence on the probability of the detection of deflected beams. The chief motivation of the current paper is to analyze a pulsar-Kerr SMBH system to see if the detection probability estimates obtained for a nonrotating SMBH are significantly different, and especially whether they might improve the prospects for near-term detection. A second purpose of this paper is to check whether the SMBH spin would have a strong enough effect on pulsar timing that spin information could be extracted from the arrival times of the pulses in a deflected beam.

The paper is organized as follows: in Section 2, we give an overview of the previous work and redefine terms that will be useful for purposes of generalization and comparison. We compare deflection of beams by a rotating SMBH and that by a nonrotating SMBH in Section 3. Section 4 describes the geometry of the system: beams emitted from a pulsar revolving around a spinning SMBH. This Section also outlines the scheme for calculating probabilities for a detection. Section 5 compares the range of detection of deflected beams in a pulsar/spinning-SMBH system to that for a pulsar/Schwarzschild-SMBH system. Section 6 compares the pattern of pulse times of arrival in the two scenarios. We conclude in Section 7. Throughout the paper, we will use the natural units ($c = 1, G = 1$) and describe distances and time in terms of the black hole mass M .

2. Review of the Schwarzschild case

As observed in Paper III, for a pulsar revolving around a Schwarzschild SMBH, there is a ‘region of detectability’ - a range of Earth angular positions on the pulsar sky at which both direct and deflected beams are detectable. We start by reviewing the determination of this region.

Figure 1 sketches the trajectory of photons outside a Schwarzschild black hole. Also illustrated is the set of angles we use to describe a particular trajectory. Here ϕ_{in} corresponds to the angle at which the photon is emitted relative to the radially outward direction at the point of emission in a spherical coordinate system centered at the SMBH; ϕ_{out} corresponds to the angle measured relative to the same radial direction far away from the strong field region of the SMBH. Paper I relates these two angles by a function F :

$$\phi_{\text{out}} = F(\phi_{\text{in}}; r_0) \tag{1}$$

where r_0 is the pulsar-SMBH distance at the time of emission. In the absence of deflection, ϕ_{out} will be equal to ϕ_{in} .

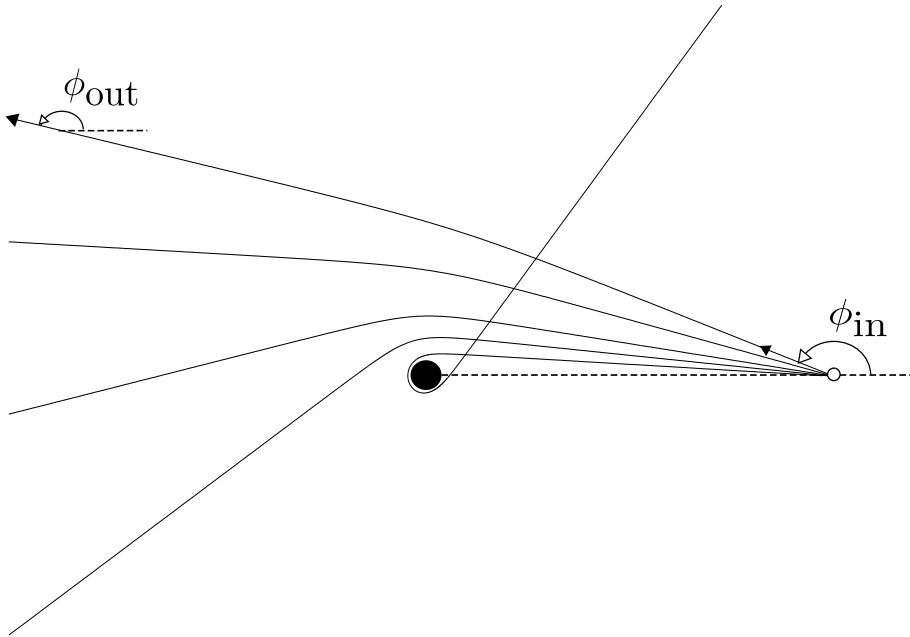


Fig. 1.— Trajectories of photons passing through the strong field region of a Schwarzschild black hole, emitted by a pulsar far away from the strong field region. Angles ϕ_{in} and ϕ_{out} are illustrated for one of the trajectories. This figure also serves for photons emitted in the equatorial plane of a spinning black hole.

Paper III notes that the intensity of a deflected beam will be modified. There is a narrow range of ϕ_{out} around $\phi_{\text{out}} = \phi_{\text{out}|\text{peak}} = \pi$ for which there is dramatic amplification corresponding to strong lensing, but in general strongly bent beams will be attenuated. Figure 2 shows the relationship of ϕ_{out} and attenuation. For $\phi_{\text{out}} \lesssim \phi_{\text{out}|\text{peak}}$ the bending is not significant; a deflected beam will not be distinguishable from a direct beam. For $\phi_{\text{out}} \gtrsim \phi_{\text{out}|\text{peak}}$, beams that are very strongly deflected are too attenuated to be detectable. Therefore, we have a $\phi_{\text{out}|\text{max}}$, a cutoff for ϕ_{out} beyond which attenuation reduces beam intensity below telescope sensitivity. We define $\delta = \phi_{\text{out}|\text{max}} - \phi_{\text{out}|\text{peak}}$ as the range of ϕ_{out} for which the deflection is significant, but the deflected beam is still detectable. If the Earth is within this range, the strongly deflected beam will be detectable.

The determination of the probability of detection of a deflected beam then involves two steps: calculating the probability of the pulsar beams being deflected to the region of detectability, and calculating how often the Earth will lie in this region. This was achieved in Paper III for nonrotating black holes and it was found that with current pulsar population models near the Galactic center, there is a good chance of detection by a multi-year program with future telescopes. Our primary aim in the current paper is to find whether these estimates are significantly changed by a consideration of the spin of the SMBH in Sgr A*. The first step will be to find a version of Figure 2 that applies

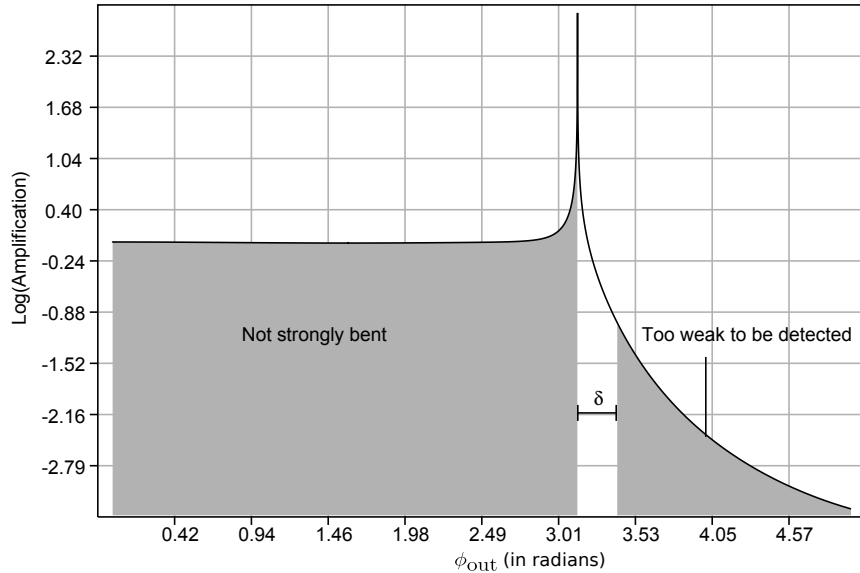


Fig. 2.— Intensity vs ϕ_{out} , for a pulsar at $100M$ from a Schwarzschild black hole. The shaded regions represent beams that are either weakly bent or too strongly attenuated.

to a spinning SMBH.

3. Expected effects of SMBH spin

The nature of the spin effects on the F function of Equation (1) are clearest for photon trajectories in the equatorial plane. Figure 1 shows sketches of such trajectories in either the Kerr geometry or the Schwarzschild geometry (for which any plane can be considered the equatorial plane). The deflection is minimum for photons emitted in the radially outward direction (i.e., for $\phi_{\text{in}} = 0$). As ϕ_{in} increases, photons get closer and closer to the black hole and deflection increases, as is evident in Figure 1. All photons straying too close, fall into the black hole. We thus identify an orbit around the black hole with the characteristic that the number of orbits of a photon traveling along this orbit grows without bound, so that ϕ_{out} effectively approaches infinity. We use the term *unstable circular orbit* (UCO) to refer to this orbit and denote the emission angle of a photon traversing this critical trajectory as $\phi_{\text{in}|\infty}$. For a Schwarzschild black hole, Figure 3 plots the relationship between ϕ_{out} and ϕ_{in} up to $\phi_{\text{in}} = \phi_{\text{in}|\infty}$. For larger values of ϕ_{in} there is no ϕ_{out} defined since these trajectories end inside the black hole.

For photons orbiting a Schwarzschild hole, it is known that the UCO lies at $r = 3M$. For those orbiting in the equatorial plane of a spinning hole, it turns out such an orbit can be obtained. We observe that for prograde photons, the size of UCO decreases as the black hole spin increases, and for retrograde photons, the size of UCO increases with the black hole spin. A smaller UCO implies

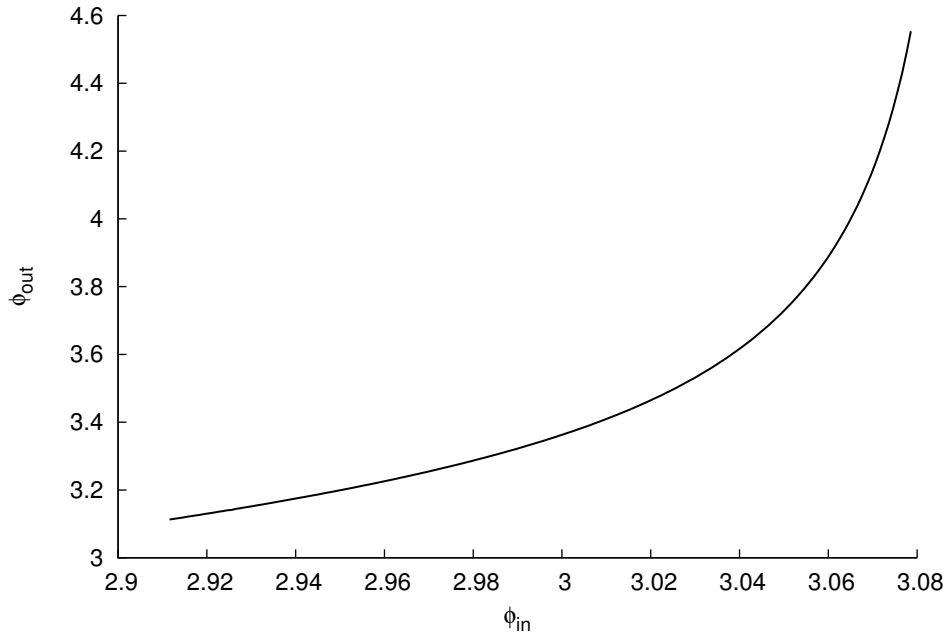


Fig. 3.— The relation of ϕ_{out} and ϕ_{in} for photons emitted at $r_0 = 100M$ from a Schwarzschild black hole.

$\phi_{\text{in}|\infty}$ for a prograde beam outside a spinning black hole will be larger than for a nonspinning black hole. Similarly, a larger UCO for retrograde beams means its $\phi_{\text{in}|\infty}$ will be smaller than that of the Schwarzschild case.

4. Calculation of Probability

The basic geometry outside a Kerr SMBH is illustrated in Figure 4. We will use spherical coordinates $\{r, \theta, \phi\}$ centered at the black hole. In the strong field region, the region of beam bending, these will be the spatial coordinates of the Boyer-Lindquist system. Since the pulsars of interest are all very far from the SMBH compared to distance M , we can consider the spatial geometry to be flat in the neighborhood of the pulsar. In the equations below, the position of the pulsar is specified by r_i , and θ_i is the angle the pulsar makes with the black hole spin axis at the time of emission. The angles γ (the planar angle) and ψ (the axial angle), describing the direction of photon emission are defined as

$$\cos \gamma = \hat{s}_i \cdot \hat{p}(\vec{d}\vec{s}_i) \quad (2a)$$

$$\cos \psi = \hat{d}\vec{s}_i \cdot \hat{p}(\vec{d}\vec{s}_i) \quad (2b)$$

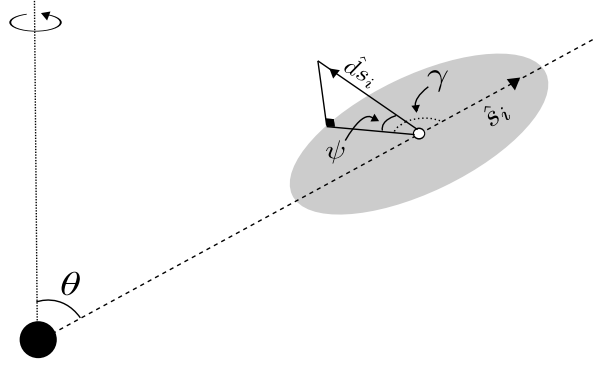


Fig. 4.— Geometry of a pulsar-Kerr system. The shaded ellipse is a disk on the plane containing the pulsar and Kerr SMBH.

where \hat{s}_i is the unit vector in the radially outward direction at the pulsar and $\hat{d}s_i$ is a unit vector denoting the initial direction of the emitted photon. The vector $\hat{p}(\hat{d}s_i)$ denotes the projection of $\hat{d}s_i$ in the orbital plane. Four integrals of the equations of motion of a photon in the Kerr geometry can be found. In Boyer-Lindquist coordinates, these are (Misner et al. 1973)

$$\rho^2 d\theta/d\lambda = \sqrt{\Theta}, \quad (3a)$$

$$\rho^2 dr/d\lambda = \sqrt{R}, \quad (3b)$$

$$\rho^2 d\phi/d\lambda = -(aE - L_z/\sin^2 \theta) + (a/\Delta)P, \quad (3c)$$

$$\rho^2 dt/d\lambda = -a(aE \sin^2 \theta - L_z) + (r^2 + a^2)\Delta^{-1}P, \quad (3d)$$

where

$$\Delta = r^2 - 2Mr + a^2, \quad (4a)$$

$$\rho^2 = r^2 + a^2 \cos^2 \theta, \quad (4b)$$

$$\Theta = \mathcal{Q} - \cos^2 \theta [-(aE)^2 + L_z^2/\sin^2 \theta], \quad (4c)$$

$$P = E(r^2 + a^2) - L_z a, \quad (4d)$$

$$R = P^2 - \Delta[(L_z - aE)^2 + \mathcal{Q}]. \quad (4e)$$

Here, r, θ and ϕ are the (Boyer-Lindquist) coordinates of the photon at different values of affine parameter λ , and $a = J/M$ is the spin parameter of the hole, where J is the angular momentum of the SMBH. The parameters L_z, E and \mathcal{Q} (Carter's constant) are the constants of motion.

Our approach will be to initialize a, r_i and θ_i . We will then use a public FORTRAN code developed by Dexter and Agol (Dexter & Agol 2009) to evaluate the trajectory of a photon through the strong field region. Along with a, r_i and θ_i , the code takes as input the three constants of motion and the final radial coordinate, which is chosen large enough that photons undergo insignificant deflection for a larger radii. The conversion from our geometric parameters to the constants of motion is outlined in the Appendix.

The code generates final polar coordinates of the photon as output. To calculate the attenuation for any given beam, we construct a circular grid of photons closely arrayed around a central photon. Using the Dexter & Agol code we then calculate the final positions of the central photon and of each photon on the grid. The ratio of the initial and final cross sectional areas of the grid of photons then gives the attenuation, indicating the change in intensity of the beam. Finally we check that the initial grid is small enough that changing to a smaller cross section does not give a substantially different result for the attenuation ratio.

5. Results: Observability of beams

To aid us in comparing pulsar-Kerr black hole system with the pulsar-Schwarzschild black hole system we introduce another set of angles η_{in} and η_{out} , illustrated in Figure 5 and defined by

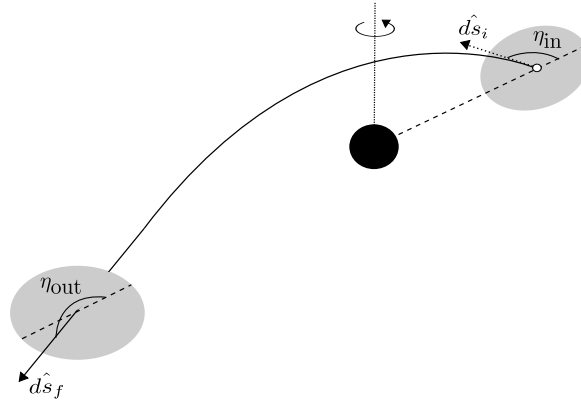


Fig. 5.— Definitions of η_{in} and η_{out} for a photon trajectory around a spinning black hole.

$$\cos \eta_{in} = \hat{s}_i \cdot \hat{d}s_i = \cos \gamma \cos \psi \quad (5a)$$

$$\cos \eta_{out} = \hat{s}_i \cdot \hat{d}s_f \quad (5b)$$

where \hat{s}_i and $\hat{d}s_i$ were defined in Section 4, and where $\hat{d}s_f$ is the spatial unit vector in the direction of the final motion of the photon far from the the pulsar-SMBH system. The interpretation of η_{in} in terms of geometric parameters γ and ψ comes from their definitions in Figure 4 and Equation (2). Far from the strong field region, $\hat{d}s_f$ and \hat{s}_f point in the same direction. Then, using Equation (1) from the Appendix for \hat{s}_i and \hat{s}_f and setting $\phi_i=0$ for simplicity, the value of η_{out} can be shown to be given by

$$\cos \eta_{out} = \cos \theta_i \cos \theta_f + \sin \theta_i \sin \theta_f \cos \phi_f . \quad (6)$$

It is expected that effects of spin of the black hole on the deflection of photons will be most prominent in the equatorial plane. As a first step in our investigation of spin effects, we will

therefore compute attenuation curves for equatorial Kerr photons similar to the curves in Equation (2). We will assume the pulsar and the photon trajectories lie in the equatorial plane of the SMBH. (In terms of our geometrical parameters, this corresponds to $\theta_i = \pi/2$ and $\psi = 0$). Figure 6 shows the η angles for this simple scenario. The definition of the η 's in this scenario is similar to the ϕ 's from the Schwarzschild case (Figure 1), and the η 's approach the ϕ 's as the black hole spin goes to zero.

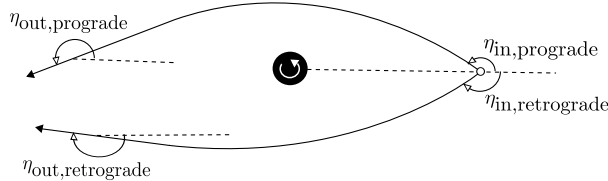


Fig. 6.— Prograde and retrograde η in the equatorial plane of a Kerr black hole.

Figure 7 plots η_{out} as a function of η_{in} for both prograde and retrograde beams emitted by a pulsar at a distance of $100 M$ from an extreme ($a = 0.99$) Kerr SMBH and compares them with the curves for a nonrotating SMBH. There is a late divergence of η_{out} for prograde photons in the near extreme Kerr SMBH case compared to the nonrotating case. This implies a larger $\eta_{\text{in}|\infty}$ for prograde Kerr beams than prograde Schwarzschild beams. Similarly, the early divergence of η_{out} for retrograde beams orbiting the near extreme Kerr SMBH implies a smaller $\eta_{\text{in}|\infty}$ for retrograde Kerr beams than retrograde Schwarzschild beams, as was observed theoretically in Section 3.

Attenuation curves are plotted in Figure 8 for the same model as in Figure 7. We notice that spin introduces a very small shift in the attenuation curve. The all-important angle δ increases by only 3% for prograde beams in the near extreme Kerr case compared to the Schwarzschild case, and there is almost exactly the same decrease in δ for the retrograde case. We also notice that as deflection increases the curves are more in agreement, η_{out} at the maximum acceptable attenuation being the same for prograde and retrograde beams in both cases, respectively. Our results show that the deviations get smaller as we go out of the equatorial plane (i.e. $\theta \neq \pi/2$ or/and $\psi \neq 0$). For larger, more relevant pulsar-SMBH distances, the differences become negligible. Thus, spin induces minimal effect on the attenuation curve of deflected beams, implying that the range of observability of deflected beams calculated for the pulsar-Schwarzschild case remains invariant for a pulsar-near extreme Kerr case. The probabilities established in Paper III of an observation with the assumption that the Sgr A* black hole is not rotating are therefore unchanged even if the black hole is spinning very rapidly.

6. Results: Timing of Pulses

The importance of beam detection lies in the potential to use deflected beams as a probe of the properties of strongly curved spacetime. For such a probe to be useful it should be sensitive

to SMBH spin. We have seen that SMBH spin has a negligible effect on beam detectability. It is therefore important to ask whether the effect of spin on pulsar beams is so slight that pulsar timing cannot be used to detect and measure spin.

We aim here only for an order of magnitude demonstration, so we make several simplifying assumptions. First, we assume that the pulsar is in a circular orbit around the SMBH, and that the pulsar beam is confined to the equatorial plane. The timing analysis of TOAs in this case has been thoroughly analyzed in Paper I for a nonspinning SMBH. In that analysis it was shown that there are two relativistic effects on pulsar TOAs. First there is the timing issue directly connected to the deflection. If the pulsar spins (relative to distant stars) at ω , then beams that will arrive at Earth without strong deflection are pulsed at frequency ω . Strongly deflected beams, on the other hand must be aimed approximately toward the SMBH, and hence, for pulsar orbital angular frequency Ω , are emitted approximately at frequency $\omega \pm \Omega$. The spin of the SMBH will have a small effect on this frequency, since it will affect the precise near-SMBH “target” towards which the to-be-deflected beam must be aimed. For simplicity we will ignore this small geometric effect, and will consider only the second relativistic effect on TOAs, the effect on the time of travel for a photon in a deflected beam.

Since the Earth is nearly stationary, a pulse emitted from a particular orbital position of the pulsar, and received at the Earth, has a unique η_{out} : the angle of the final direction of the beam with respect to the radially outward direction through the pulsar at the time of emission in a spherical coordinate system centered at the Galactic center (defined in Equation (5), and pictured in Figure 5). For \mathcal{T} , the pulse arrival time, $d\mathcal{T}/d\eta_{\text{out}}$ is then a measure of variation in arrival times as the pulsar travels through its orbit. For a circular orbit, the radially outward direction through the pulsar rotates at a fixed rate, the angular velocity Ω of the pulsar orbit. In the absence of strong gravity effects, $d\mathcal{T}/d\eta_{\text{out}}$ would then be a constant. Any deviation from a constant value is therefore a direct measure of strong gravity effects, and we use this rate to investigate the sensitivity of TOAs to SMBH spin.

The change in coordinate time as a pulse traverses the SMBH and reaches the Earth is given by

$$\mathcal{T}(\eta_{\text{out}}; R) = 2 \int_{r_{\text{min}}}^{r_0} J(r) dr + \int_{r_0}^R J(r) dr \quad (7)$$

where r_0 is the pulsar-SMBH distance, R is the distance between the SMBH and the Earth and

$$J(r) = \frac{dt}{dr} = \frac{P(r^2 + a^2)\Delta^{-1} + aL_z}{\sqrt{R}} \quad (8)$$

is obtained from the equations of motion of a photon in the Kerr geometry (Equations (3) and (4)). Since the Earth is very far away from the pulsar-SMBH system, we use Equation (7) to find the value of \mathcal{T} to a distance R much larger than M , where relativistic effects are negligible.

To compare the prograde and the retrograde pulses for a possible spin signature, we start with the absolute value of $d\mathcal{T}/d\eta_{\text{out}}$ as a measure of the variation in the TOA. We analyze $d\mathcal{T}/d\eta_{\text{out}}$

as a function of the absolute value of η_{out} , an indicator of the orbital position of the pulsar. If the SMBH is not rotating, the prograde and the retrograde beams will suffer identical deflection and we find that this Schwarzschild value $d\mathcal{T}/d\eta_{\text{out}}|_S$ is, of course, the same in the prograde and the retrograde cases for any η_{out} . If the SMBH is rotating, this symmetry is broken; there will be different values of $d\mathcal{T}/d\eta_{\text{out}}$ for prograde and retrograde orbits. We use the absolute value of $d\mathcal{T}/d\eta_{\text{out}} - d\mathcal{T}/d\eta_{\text{out}}|_S$ as a measure of the spin detectability.

This measure, and all measures of deflection, depend on the closest approach of the pulsar beam to the SMBH, and that closest-approach distance determines the attenuation of the TOAs. We choose, therefore, to compare the prograde and retrograde values of $d\mathcal{T}/d\eta_{\text{out}}$ for fixed, relevant values of the attenuation of the pulsar beam. Table 1 gives the result for 50% attenuation, i.e., for significant deflection, and for 90% attenuation, i.e., for the limiting deflection, the deflection beyond which attenuation is assumed to preclude observation. The tabulated values are absolute values of $d\mathcal{T}/d\eta_{\text{out}} - d\mathcal{T}/d\eta_{\text{out}}|_S$. This value is the same for the prograde and retrograde cases. In the two cases the signs are opposite, so the total prograde/retrograde difference is twice the values tabulated. Several properties of spin effects are immediately clear from the tables: the spin-induced effect, at any attenuation, is proportional to the SMBH spin; the effect depends very weakly on the pulsar-SMBH distance; the effect is stronger at the stronger deflection of the 90% deflection, but the sensitivity to deflection is not strong.

50% atten.	pulsar-SMBH distance			90% atten.	pulsar-SMBH distance		
SMBH spin	$10^2 M$	$10^3 M$	$10^4 M$	SMBH spin	$10^2 M$	$10^3 M$	$10^4 M$
0.30	0.023	0.020	0.019	0.30	0.028	0.025	0.024
0.60	0.046	0.040	0.038	0.60	0.056	0.049	0.048
0.99	0.075	0.067	0.063	0.99	0.093	0.081	0.079

Table 1: The value of $d\mathcal{T}/d\eta_{\text{out}} - d\mathcal{T}/d\eta_{\text{out}}|_S$, at two different attenuations. Values are given in units of the SMBH mass M for two different attenuations. The values are listed for various spin parameters and pulsar-SMBH distance.

For our central SMBH with a mass close to $4 \times 10^6 M_\odot$ (Gillessen et al. 2009; Ghez et al. 2008), these differences are on the order of 1 second. The pulsars close to the Galactic center are expected to be spinning at rates of order 1 second, thus the spin effects would induce a phase shift on the order of one cycle. These effects, furthermore, originate in the portion of the photon orbit close to the SMBH, so this order of difference is maintained even for larger, more relevant values of pulsar-SMBH distance. The conclusion, based on our limited analysis, is that pulsar timing of deflected pulses detected at the Earth would be able to extract the spin signatures of the Sgr A* SMBH.

This estimate is of course for an oversimplified picture. To get closer to an accurate prediction, we must consider more general models. A particularly important part of such an analysis would be an effect that, like spin, induces different delays for prograde and retrograde beams: the eccentricity

of the orbit. Preliminary calculations suggest that the pattern of timing effects due to eccentricity of pulsar orbit is, in fact, distinct from the pattern introduced by the SMBH spin.

7. Conclusion

The detection and analysis of pulsar beams strongly deflected by the SMBH in Sgr A* holds promise of providing a tool for probing strongly curved regions of spacetime. An important question has been the probability that such beams are detectable. To remedy a shortcoming of earlier estimates of such probability, we have considered here whether the spin of the Sgr A* SMBH can have a significant effect on detectability. We have found that even for the conditions in which spin should have its greatest effects (equatorial photon trajectories, near extreme rotation) the effect of spin on detectability is negligible.

While the effect on detectability is negligible, we have demonstrated that the effect of spin on pulsar arrival times is significant enough that these beams, if detected, can provide us a way of determining the spin of the SMBH. The fact that this determination is well within the precision of pulsar timing suggests that the timing can also determine whether the spacetime near the Galactic center deviates from the Kerr geometry. The motivation for an observational program therefore remains strong.

We gratefully acknowledge support by the National Science Foundation under grants AST0545837 and HRD0734800. We also thank the Center for Gravitational Wave Astronomy, the Center for Advanced Radio Astronomy, and the Department of Physics and Astronomy at the University of Texas at Brownsville.

Appendix: Constants of motion from geometrical parameters

We work in a spherical coordinate system centered at the black hole. As argued before, the pulsars are far enough from the black hole for us to assume the spacetime is flat there. From Figure 4 we then have

$$\vec{s} = r \cos \theta \hat{z} + r \sin \theta \cos \phi \hat{x} + r \sin \theta \sin \phi \hat{y}, \quad (1)$$

from which we find

$$\begin{aligned} \vec{ds}_i &= (\cos \theta_i dr - r_i \sin \theta_i d\theta) \hat{z} \\ &+ (\sin \theta_i \cos \phi_i dr + r \cos \theta_i \cos \phi_i d\theta - r_i \sin \theta_i \sin \phi_i d\phi) \hat{x} \\ &+ (\sin \theta_i \sin \phi_i dr + r_i \cos \theta_i \sin \phi_i d\theta + r_i \sin \theta_i \cos \phi_i d\phi) \hat{y} \end{aligned} \quad (2)$$

and

$$\begin{aligned} \vec{p}(\vec{ds}_i) &= \cos \theta_i dr \hat{z} + (\sin \theta_i \cos \phi_i dr - r_i \sin \theta_i \sin \phi_i d\phi) \hat{x} \\ &+ (\sin \theta_i \sin \phi_i dr + r_i \sin \theta_i \cos \phi_i d\phi) \hat{y} \end{aligned} \quad (3)$$

where r_i, θ_i and ϕ_i are coordinates of the photon at the time of emission in a spherical coordinate system centered at the black hole. The initial choice of ϕ is arbitrary; we set $\phi_i=0$ for simplicity. The above equations and Equations (2) give us

$$\cos \gamma = \frac{\vec{s}_i \cdot \vec{p}(\vec{ds}_i)}{|\vec{s}_i| |\vec{p}(\vec{ds}_i)|} = \frac{dr}{\sqrt{(dr)^2 + (r_i \sin \theta_i d\phi)^2}} \quad (4)$$

so that

$$\tan \gamma = r_i \sin \theta_i \left(\frac{d\phi}{dr} \right)_i . \quad (5)$$

From those equations we also have

$$\begin{aligned} \cos \psi &= \frac{\vec{ds}_i \cdot \vec{p}(\vec{ds}_i)}{|\vec{ds}_i| |\vec{p}(\vec{ds}_i)|} \\ &= \frac{(dr)^2 + (r_i \sin \theta_i d\phi)^2}{\sqrt{(dr)^2 + (r_i d\theta)^2 + (r_i \sin \theta_i d\phi)^2} \sqrt{(dr)^2 + (r_i \sin \theta_i d\phi)^2}}, \end{aligned} \quad (6)$$

from which it follows that

$$\tan \psi = \frac{r_i d\theta}{\sqrt{(dr)^2 + (r_i \sin \theta_i d\phi)^2}} = \frac{r_i d\theta}{\sqrt{(dr)^2 + (\tan \gamma dr)^2}} \quad (7)$$

and finally

$$\tan \psi = r_i \cos \gamma \left(\frac{d\theta}{dr} \right)_i . \quad (8)$$

By specifying γ, ψ and initial values of r and θ , we obtain initial values of $d\phi/dr$ and $d\theta/dr$ which we then use to solve Equations (3) and find the constants of motion.

REFERENCES

- Baganoff, F. K., Maeda, Y., Morris, M., et al. 2003, ApJ, 591, 891
- Broderick, A. E., Fish, V. L., Doeleman, S. S., & Loeb, A. 2009, ApJ, 697, 45
- Dexter, J., & Agol, E. 2009, ApJ, 696
- Doeleman, S. S., Weintroub, J., Rogers, A. E. E., et al. 2008, Nature, 455, 78
- Faucher-Giguère, C.-A., & Kaspi, V. M. 2006, ApJ, 643, 332
- Genzel, R., Schödel, R., Ott, T., et al. 2003, Nature, 425, 934
- Ghez, A. M., Salim, S., Weinberg, N. N., et al. 2008, ApJ, 689, 1044
- Gillessen, S., Eisenhauer, F., Trippe, S., et al. 2009, ApJ, 692

- Levin, Y. 2006, MNRAS, 374, 515
- Liu, S., & Melia, F. 2002, ApJ, 573, L23
- Maness, H., Martins, F., Trippe, S., et al. 2007, ApJ, 669, 1024
- Misner, C. W., Thorne, K. S., & Wheeler, J. A. 1973, Gravitation (W. H. Freeman and Company)
- Muno, M. P., Pfahl, E., Baganoff, F. K., et al. 2005, ApJ, 622, L113
- Nayakshin, S., & Sunyaev, R. 2005, MNRAS, 364, L23
- Pfahl, E., & Loeb, A. 2004, ApJ, 615, 253
- Porquet, D., Predehl, P., Aschenbach, B., et al. 2003, A&A, 407, L17
- Schödel, R., Ott, T., Genzel, R., et al. 2002, Nature, 419, 694
- Stovall, K., Creighton, T., Price, R. H., & Jenet, F. A. 2012, ApJ, 744
- Wang, Y., Creighton, T., Price, R. H., & Jenet, F. A. 2009a, ApJ, 705
- Wang, Y., Jenet, F. A., Creighton, T., & Price, R. H. 2009b, ApJ, 697

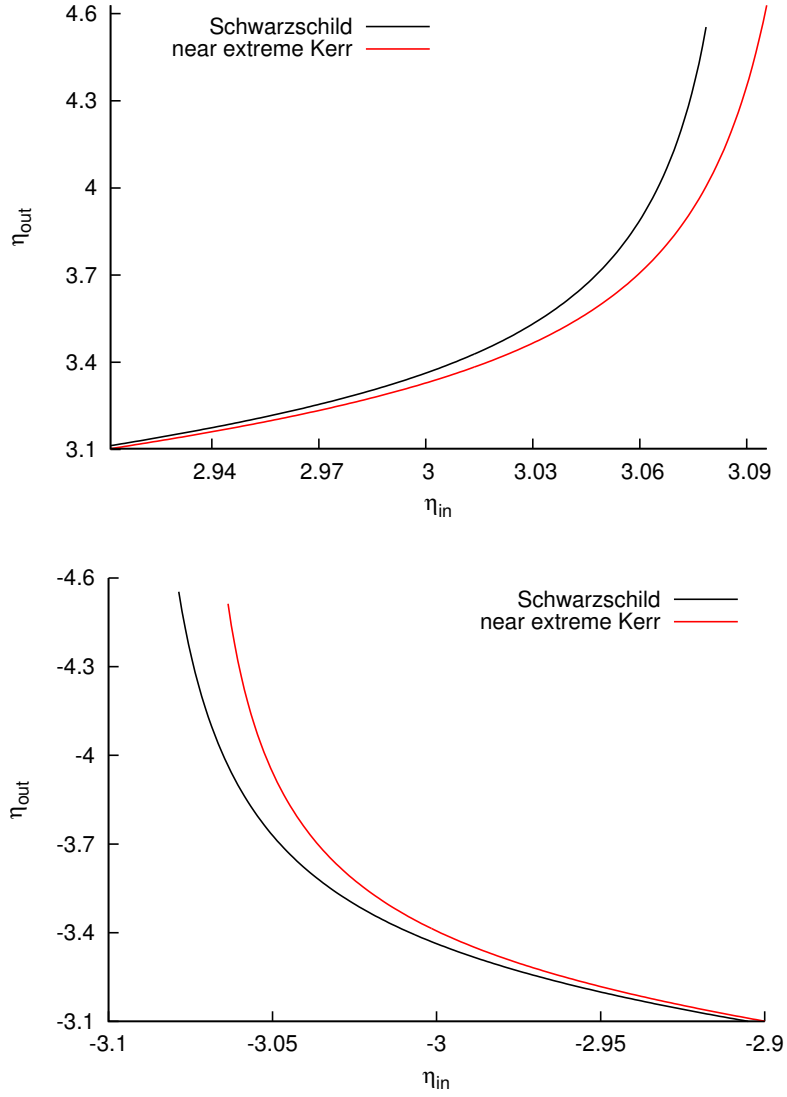


Fig. 7.— The relationship of η_{out} and η_{in} . The top figure shows prograde beams in the equatorial plane of an $a = 0.99$ SMBH (red) and Schwarzschild SMBH (black); the bottom figure shows the same comparison for retrograde beams.

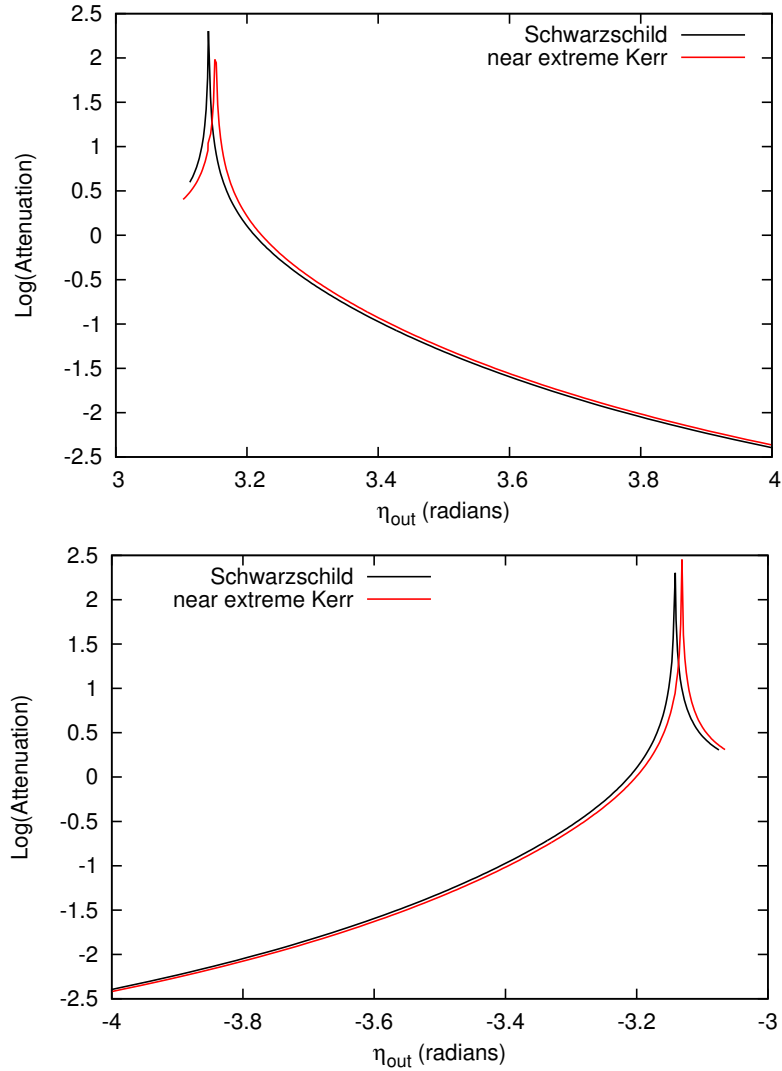


Fig. 8.— Attenuation of pulse intensity as a function of η_{out} for the same models as in Figure 7. The top figure shows the comparison of the Schwarzschild curve with the prograde case, the bottom with the retrograde case.